Biosensing and Actuation for Microbiorobots

M. Selman Sakar*, Edward B. Steager*, A. Agung Julius‡, MinJun Kim†, Vijay Kumar*, and George J Pappas*

Fig. 1. Fabrication processes of the microstructures with APTES coating.

I. ABSTRACT

In this paper, we describe how signaling networks and actuation in bacterial cells and biomolecular networks of bacteria can be used to develop an integrated micro-bio-robotic system. SU8 microstructures blotted with swarmer cells of *Serratia Marcescens* in a monolayer are propelled by the bacteria in the absence of any environmental stimulus. We call such microstructures with bacteria *Micro Bio Robots* (MBRs) and the uncontrolled motion in the absence of stimuli *self actuation*. Our paper has two primary contributions. First, we demonstrate the control of MBRs using self-actuation, DC electric fields and ultra-violet radiation, and develop experimentally validated mathematical model for the MBRs. This model allows us to use self-actuation and electrokinetic actuation to steer the MBR to any position and orientation in a planar micro channel. Second, we describe the development of biosensors for the MBRs. This is done by attaching genetically engineered *Escherichia coli* cells that are capable of sensing nonmetabolizable lactose analog methyl-β-D-thiogalactoside (TMG). We describe the fabrication process for MBRs and show experimental results demonstrating sensing, actuation and control.

Keywords: microactuation, biological systems, flagellated bacteria, micromanipulation, biosensing.

II. INTRODUCTION

There is extensive ongoing research on developing artificially engineered micro/nanoscale structures with novel approaches of microactuation and sensing [1]–[10]. There is relatively less work on exploiting naturally-ocurring biomolecular motors for actuation of micro and nano structures. The use of microorganisms to produce useful work has been previously demonstrated by a number of different groups [11]–[14]. The potential for developing micro-robots powered by biomolecular motors has been demonstrated by several researchers [15]–[18].

Biological systems have signaling networks which respond to chemicals in the environment. In recent years, increased emphasis has been placed on employing the inherent chemical recognition properties of biological systems in the development of biosensors. Cell-based biosensors are portable devices that contain living biological cells. These biosensors monitor physiological changes induced by exposure to environmental perturbations such as toxicants, pathogens, or other agents [19]. Our own work addresses the use of *E.coli* as a biosensor for sensing lactose (or a nonmetabolizable analog, methyl-β-D-thiogalactoside) via a regulatory network responsible for lactose induction and the development of a stochastic hybrid model of this system [20].

Our paper builds on our previous work [21] on bacterial actuation, exploiting signaling networks in individual cells and biomolecular networks of bacteria to develop an integrated micro-bio-robotic system. SU8 microstructures blotted with swarmer cells of *Serratia marcescens* in a monolayer are propelled by the bacteria in the absence of any environmental stimulus. We call these microstructures with bacteria *Micro Bio Robots* (MBRs) and the uncontrolled motion *self actuation*. Our paper has two primary contributions. First, we demonstrate the control of MBRs using self-actuation, DC electric fields and ultra-violet radiation and develop an experimentally validated mathematical model for the MBRs. This model allows us to to steer the MBR to any position and orientation in a planar micro channel using visual feedback using an inverted microscope. Second, we describe the development of biosensors for the MBRs. This is done by attaching genetically engineered *Escherichia coli* cells that are capable of sensing nonmetabolizable lactose analog methyl-β-D-thiogalactoside (TMG). This proof-of-concept prototype is based on similar designs of biosensors on MBRs for sensing a variety of analytes such as heavy metals (i.e., copper), metabolites (i.e., sugars), carcinogens, and stress inducers (i.e., antibiotics) [19]. In addition to these two main contributions, our paper reports on details of the fabrication process for MBRs that have heterogenous populations of bacteria, *S. marcescens* and *E. coli*, attached in monolayers for the first time.

III. MATERIALS AND METHODS

A. Fabrication of patterned microstructures

The SU8 microstructures are patterned on 43 × 50 mm glass slides with a thickness of 170 μm (No. 0). The

*GRASP Laboratory, School of Engineering and Applied Sciences, University of Pennsylvania, Philadelphia, PA 19104, U.S.A. `sakarmah,esteager,kumar,pappasg@seas.upenn.edu`
†Department of Mechanical Engineering and Mechanics, Drexel University, Philadelphia, PA 19104, U.S.A. `mkim@coe.drexel.edu`
‡Department of Electrical, Computer and Systems Engineering, Rensselaer Polytechnic Institute, Troy, NY 12180, U.S.A. `agung@ecse.rpi.edu`
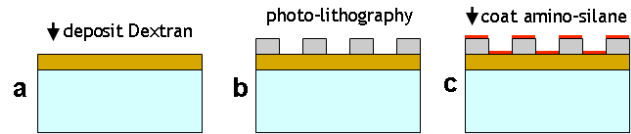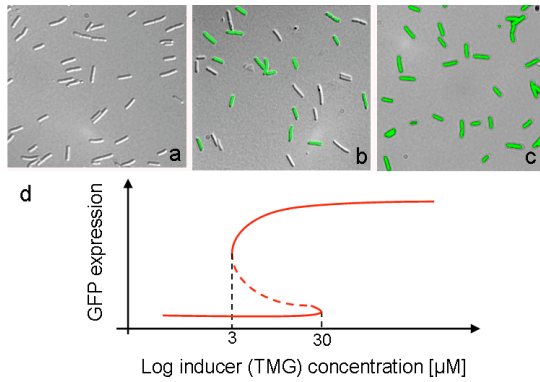
Fig. 2. Overlayed green fluorescence and inverted phase-contrast images of cells that are initially uninduced for lac expression, then grown for 20 h in a solution with (a) no TMG (b) 10 μM TMG (c) 100 μM TMG (d) Steady-state solutions of the system. The induced state is shown as the upper dark line whereas the uninduced state is shown as the lower dark line. The intermediate unstable steady state is shown as a dashed line.

fabrication sequence is shown in Figure 1. For the details of fabrication process, we refer to [22]. Microstructures are automatically released when exposed to any source of water.

B. Bacterial strains, growth conditions and media

The Green Fluorescent Protein (GFP) gene under the control of the wild-type lac promoter was inserted into the chromosome of *E. coli* by van Oudenaarden and co-workers to produce the strain we used in our experiments. The details of the transformation is explained in [23]. *E.coli* cells were grown at 37°C in M9 minimal medium with succinate as the main carbon source. To obtain the fluorescence images of bacteria (Figure 2 a-c), cells were grown overnight in the absence of TMG. Afterwards, cells were transferred from this initial culture into media containing specified amounts of TMG (0 μM, 10 μM and 100 μM). The microscope slides with agarose pads were prepared using the protocol described in [24]. These pads press the cells against the surface of a cover glass and force the cells onto a single plane. Immobilization ensures that the cells do not move between subsequent measurements of the same group of cells.

The bacteria *Serratia marcescens* are cultured using a swarm plate technique as described in [11]. Cells were transferred into microfluidic channels by pipetting 500 μl of motility buffer (0.01 M potassium phosphate, 0.067 M sodium chloride, 10-4 M ethylenediaminetetraacetic acid, and 0.002% Tween-20, pH 7.0) onto the leading edge of the swarm plate and pipetting back. For the experiments in which electric fields were applied to MBRs, bacteria were attached by blotting microstructures directly along the active swarm edge.

C. Bacterial monolayers

The pink slime produced by swarmer cells of S. marcescens allows them to stick to the surface of the

microstructures naturally. However, a special surface treatment is needed order to attach our *E. coli* cells to SU-8 microstructures. By coating the surface with APTES or (3-aminopropyl)triethoxysilane, a positively charged surface was created where negatively charged bacteria cells can be electrostatically immobilized [25]. The deposition of APTES (Sigma Aldrich 440140) molecules was carried out by immersion of the substrate into a freshly prepared solution containing APTES molecules diluted at 3% with ethanol for 1 hour; the slide was then rinsed with ethanol, dried under nitrogen stream, and heated on a 90°C plate for 5 min (Figure 1c).

D. Fabrication of experimental chamber

All experiments were conducted in a polydimethylsiloxane (PDMS) chamber on a 50×50 mm^2 glass plate. For details of fabrication process and the connection diagram, please refer to [22]. The control chamber was filled with motility buffer. The voltage on the electrodes is applied using two programmable power supplies (Agilent E3631A) which are connected to a desktop computer (Dell Precision T3400) via a RS-232 serial port.

E. Fabrication of microfluidic channels

Microfluidic devices were manufactured in PDMS by using soft lithographic techniques as described [26]. Briefly, a high resolution printer was used to generate a mask (in the form of a transparency) from a CAD file. A negative master, consisting of patterned SU-8 photoresist on a silicon wafer was fabricated and used to make molds of PDMS. Holes, which served as inlets and outlets, were reamed through the top of the PDMS molds by using syringe needles.

The microchannel was 5 mm long, 1 mm wide, and 50 μm deep. The fabricated PDMS mold was brought into conformal contact with a 43x50 mm glass slide on which the microstructures were patterned and the assembly was heated on top of a hot plate at 80°C for 2 hours to form a reversible bond. The channel was filled with a suspension of cells.

IV. CONTROL OF MBRS

A. Model for self-actuation

There are two approaches to actuating a MBR. As explained in [21], *self-actuation* is due the random swimming and tumbling action of individual cells. The second source of actuation is electrokinetic. Because bacteria are charged, an electric field exerts an electrostatic Coulomb force on the particles. Thus the individual bacteria and therefore the MBR exhibit electrophoresis.

In [21], we showed that the MBR under self-actuation can be modeled by a stochastic, kinematic model:

$$\frac{dr}{dt} = \frac{1}{k_T}\{\sum_{i=1}^{N_b} p_i(t)n_i\}, \tag{1a}$$

$$\frac{d\phi}{dt} = \frac{1}{k_R}\{\sum_{i=1}^{N_b} p_i(t) \cdot (b_{i,x}\sin\theta_i - b_{i,y}\cos\theta_i) \tag{1b}$$
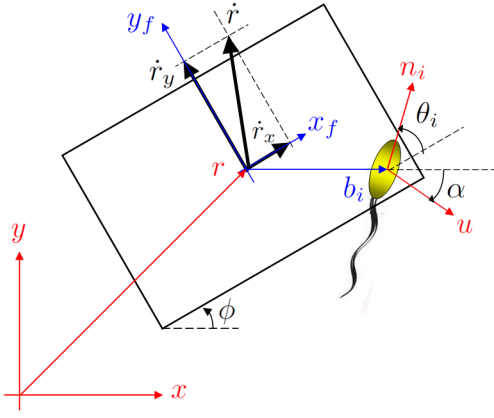
Fig. 3. A schematic of an MBR. The angle α is formed by the main axis of the MBR and the x axis. The vector $\mathbf{r}$ denotes the position of the MBR's center of mass. The vector b_i denotes the position of the i-th bacterium w.r.t the MBR's center of mass. The vector ψ_i is a unit vector that denotes the orientation of the i-th bacterium. The angle θ_i is formed by the MBR's main axis and the orientation of the i-th bacterium.

where N_b denotes the number of bacteria in the MBR, the position of the i-th bacterium with respect to the center of mass of the MBR is denoted by the vector $\mathbf{b}_i = (b_{i,x}, b_{i,y})$ in the body-fixed coordinate frame, the orientation of the bacterium is characterized by the angle θ_i, and (r, ϕ) denote the position and orientation of the MBR in a world frame as shown in Figure 3. We denote the time-varying propulsive force provided by the i-th bacterium as $p_i(t)$ acting along a preferred axis n_i. Inherent in this model is the assumption that the inertial forces are negligible and that the propulsion by the bacteria is balanced by drag forces that are linearly proportional to velocity. Because the Reynolds number for the system (the barge as well as the individual bacteria) is much less than 1, this is a very reasonable assumption. k_T is the translational viscous drag coefficient, and k_R is the rotational viscous drag coefficient.

Assuming that the switching behavior of each flagellum is an independent Poisson process, the behavior of each bacterium can be modeled as continuous-time Markov chain with two states, *run* and *tumble* [27]. Thus $p_i(t)$ can be modeled as a Poisson process with known statistics [21]. We further assume that the bacteria are independent, in spite of observations that suggest that bacteria might be hydrodynamically or physically coupled. Finally we assume that the processes $p_i(t)$ reach their steady state very quickly allowing us to derive the expected values of the velocities in Equation (1):

$$Ev_x = \frac{\bar{p}}{k_T} \sum_{i=1}^{N_b} \cos\theta_i, \ \ Ev_y = \frac{\bar{p}}{k_T} \sum_{i=1}^{N_b} \sin\theta_i. \quad (2)$$

$$E\omega = \frac{\bar{p}}{k_R} \sum_{i=1}^{N_b} (b_{i,x}\sin\theta_i - b_{i,y}\cos\theta_i). \quad (3)$$

Remarkably, the expected velocities of the stochastic pro-

cess is characterized by only three parameters:

$$\beta_1 := \frac{1}{k_T} \sum_{i=1}^{N_b} \cos\theta_i, \quad (4)$$

$$\beta_2 := \frac{1}{k_T} \sum_{i=1}^{N_b} \cos\theta_i, \quad (5)$$

$$\beta_3 := \frac{1}{k_R} \sum_{i=1}^{N_b} (b_{i,x}\sin\theta_i - b_{i,y}\cos\theta_i). \quad (6)$$

It is worth noting that these parameters depend on the number of bacteria and their spatial distribution on the MBR. Because these parameters appear linearly in the model, the identification of these parameters from experimental data is straightforward. $\beta_{1,2,3}$ summarize the distribution of the bacteria on the microstructure. In [21], we showed that this mathematical model is able to predict the behavior of the system in the absence of external stimuli very well.

B. Model for electrokinetic actuation

In order to develop a model for electrophoresis, two sets of experiments were performed. First, the SU8 microstructures were tested in the experimental chamber without bacteria attached using DC electric fields ranging from 1-10 V/cm. For the electric fields applied during these experiments, the structures demonstrated no movement that might be expected due to electrokinetic effects. In the next set of experiments, electric fields ranging from 1-10 V/cm were applied to the MBRs. They responded by immediately seeking the positive electrode with a directed movement that was primarily translational, but also includes some rotation because of *self actuation*. Upon switching the polarity of the system, the motion immediately reversed direction.

To investigate the fundamental electrokinetics of the microbiorobot, several trials were performed by measuring velocity versus electric field. This investigation yielded a linear relationship between the two parameters reflective of electrophoretic movement. Thus, the detailed motion of the microbiorobot could be accurately modeled by a sum of the movement due to the self-coordinating, unstimulated movement and electrophoretic movement. Indeed, surface patterning of bacteria imparts a charge that leads to a direct mechanism of translational control of the MBR.

We now extend the model of [21] to incorporate electrokinetic actuation (See Figure 3). If each of the N_b bacteria in the MBR is subject to the same electric field, we arrive at the stochastic kinematic model:

$$\frac{dr}{dt} = \frac{1}{k_T}\{\sum_{i=1}^{N_b} p_i n_i + N_b(\epsilon_C|E|)u\}, \quad (7a)$$

$$\frac{d\phi}{dt} = \frac{1}{k_R}\{\sum_{i=1}^{N_b} p_i \cdot (b_{i,x}\sin\theta_i - b_{i,y}\cos\theta_i) +$$

$$(\epsilon_C|E|)\sum_{i=1}^{N_b} (b_{i,x}\sin(\alpha-\phi) - b_{i,y}\cos(\alpha-\phi))\}. \quad (7b)$$

where the strength of the electric field is denoted by $|E|$ and u is the unit vector that represents the direction of the electrophoretic force exerted on each bacterium. The strength of the electrophoretic force is given by $\epsilon_C|E|$ where ϵ_C is a constant related to the charge of the cell body.

Experimental observations suggest that the angular velocity of the MBR is not modulated by the application of the electrical fields. In other words, the observed angular velocity with the application of electrical fields was indistinguishable from the angular velocity under self-actuation. We concluded that because of the random orientation and distribution of bacteria, the moments due to the applied electric field must be zero. In other words,

$$\sum_{i=1}^{N_b} (b_{i,x}\sin(\alpha - \phi) - b_{i,y}\cos(\alpha - \phi)) = 0 \qquad (8)$$

This simplifies the model. The expected velocities can be derived from the stochastic kinematic model:

$$Ev_x = \beta_1\bar{p} + \beta_4 u_x \qquad (9)$$
$$Ev_y = \beta_2\bar{p} + \beta_4 u_y \qquad (10)$$
$$E\omega = \beta_3\bar{p} \qquad (11)$$

where $\beta_4 = (1/k_T)N_b\epsilon_C$ is experimentally determined via linear regression from experimental data.

The comparison of the experimental observations with theoretical predictions is shown for a representative experiment in Figure 4 with a 40×40 μm square MBR with the parameters β_1 = - 5 $\mu m/s/pN$, β_2 = -7 $\mu m/s/pN$, β_3 = -1.4 $rad/s/pN$, and β_4 = 0.56 $\mu m/s/V/cm$. During the experiment, $20V/cm$ is applied to the MBR is $-y$ direction. One shortcoming of the model that may explain the slight deviation in terms of linear velocities between predictions and experiments is our implicit assumption of symmetry when calculating the drag force. Our drag coefficients k_T and k_R are independent of the orientation of the MBR. We are currently developing a detailed analytical model of the drag force acting on a square plate moving parallel to a surface in a low Reynolds number regime and this may yield an even better match with the data.

V. RESULTS

A. Experimental Setup

Imaging was performed on a Leica DMIRB inverted microscope using both phase contrast and fluorescence. Images were captured using a high-speed camera (MotionPro X3, Redlake) with a frame rate of 30 frames/s. A simple tracking algorithm was designed to feedback the position and orientation of the MBR in the motility buffer [21].

Exposure to UV light has been established as a mechanism which affects the motility of bacteria. Since MBRs are self-actuated in the absence of external stimuli, use of UV light exposure is an effective means for stopping the motion due to self actuation [18]. The optical path included a 100 W mercury light source and a 63 X Fluorotar objective. The bacterial flagella gradually de-energize during exposure
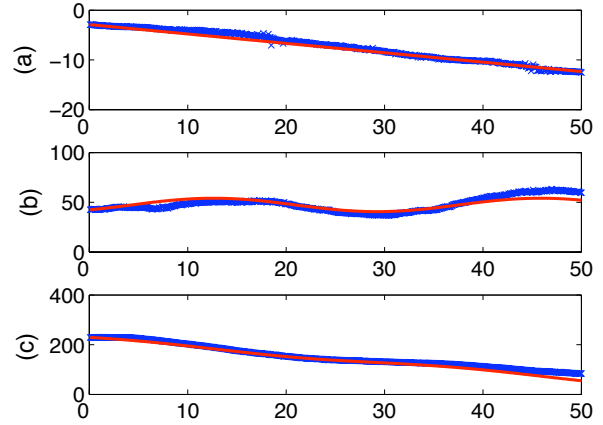

Fig. 4. The comparison between the experimental data (blue line) and the model prediction (red line)for a square MBR (40 μm × 40 μm). (a) ϕ in rad, (b) x in μm, (c) y in μm

while the magnitude of the angular velocity of the MBRs decreases exponentially. The rotational motion completely ceases after 50 s. This characterization was used to adjust angular orientation of MBRs for transporter experiments.

B. Micromanipulation

To demonstrate the combination of control techniques (UV light and EFs), MBRs were used to engage and transport a 10μm cube composed of SU8 epoxy, referred to here as the target (see Supporting Video). Based on the water-soluble sacrificial release method, several targets were released into the experimental cell. MBR transporters were also released and actively moving in the experimental cell due to self actuation.

An MBR/target pair was selected and a path was planned for the translational and rotational motion. First, the transporter was moved to the vicinity of the target by adjusting the electric field along the two major axes (Figure 5). The field employed was roughly 10 V/cm. When the transporter was within 100 μm of the target cube, a dose of UV light was applied to stop the rotational motion of the structure. When the target was engaged, changes in orientation were caused not by propulsion from the flagellar motors, but from reaction forces between the transporter and the target.

Targets were moved several hundred microns by further applying electric fields. Despite the fact that the flagellar motors of the bacteria were disabled, the electric field still moves the transporter and in turn, the target.

C. Biosensing experiments

In the previous section we showed how visual feedback can be used to drive the system to a desired position and orientation. In this section, we describe a novel approach to use "on-board" sensing to steer the MBRs to chemically or biologically relevant goals. In order to dow this, we
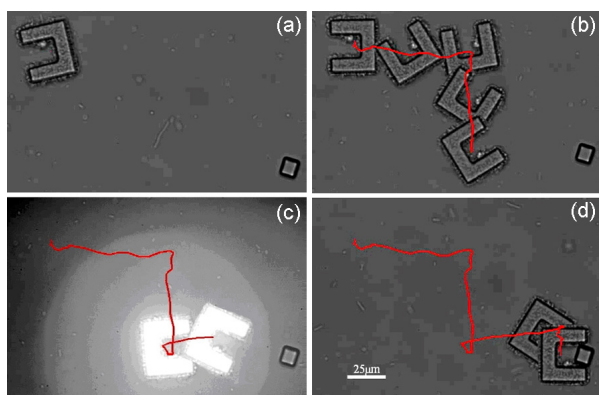
Fig. 5. Micromanipulation experiment (a) Initial position of U-shaped MBR transporter and target. (b) Transporter is moved to the right and down while rotation continues. (c) Rotation is stopped in proper orientation upon exposure to UV light. (d) Transporter engages the target object.
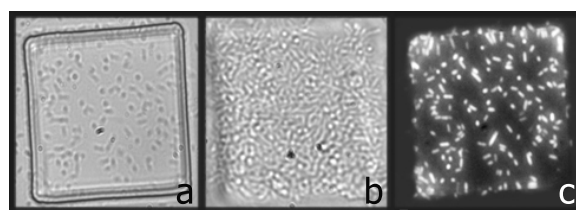

Fig. 6. (a) Phase contrast image of the microstructure showing the attached *E.coli* cells (b) Phase contrast image of a monolayer of the mixed population. *S. Marcescens* cells fill all the gaps on the microstructure. (c) Fluorescence image visualized only *E.coli* cells as they express GFP while *Serratia* cells do not.

employ two different sets of bacterial cells. The first set of bacteria are *S. marcescens* that control the motion of the MBR as before. The second set of bacteria are genetically engineered *E. coli* that act as biosensors. We briefly introduce the molecular biology necessary to understand and model the bio-sensing phenomenon and describe our fabrication technique that allows us to create monolayers with two different type of bacterial cells on our MBRs.

Lactose metabolism in *E. coli* is controlled by the lac operon, which consists of the $lacZ$, $lacY$, and $lacA$ genes encoding β-galactosidase, lactose permease ($lacY$), and acetyltransferase, respectively. Because of the positive feedback, the network is bistable. The lac genes are fully expressed for (almost) every cell in a population under high extracellular concentrations of TMG while at moderate inducer concentrations, the lac genes are highly expressed in only a fraction of a population (Figure 2d). The population heterogeneity was interpreted by Novick and Weiner as a result of the bistability of the gene expression mechanism of individual cells combined with stochastic fluctuations inherent to biomolecular processes involving few molecules [28].

In this study, we employed the same strain as biosensors carried by our MBRs so that GFP expression can be used as a readout of bacterial activity and we in effect have a transducer for the biochemicals sensed by the bacteria. In our previous work, we developed a hybrid stochastic model for the system [20]. This model captures the bistability of the biosensing system and allows us to predict the response of the system to TMG (and potentially other chemicals) in the environment.

The use of laminar flow of liquids in capillary systems to perform patterned cell deposition was described before [29]. We combined their method with our procedure of fabricating microstructures and a surface treatment described elsewhere [25] to pattern two different types of bacteria on SU-8 microstructures. These constructs are employed as mobile biosensors.

Microstructures were fabricated in such a way that they could be trapped inside our PDMS microchannel. They were silanized as described in Materials and Methods. After sealing the PDMS mold against the glass slide, the microchannel was initially filled with a suspension of *E.coli* cells for 10 min. Cells adsorbed nonspecifically to the regions of the surface over which the solutions containing them flowed. Cells that did not adhere strongly were washed away with PBS (3-min wash) and the remaining adherent cells were visualized using phase contrast microscopy (Figure 6a). The microchannel was then filled with a suspension of *S. marcescens* harvested from the swarm plate (see Materials and Methods) for 5 min followed by a 3-min PBS wash. Once again cells were visualized using phase contrast imaging (Figure 6b). With the attachment of *S. marcescens*, the microstructures started to move immediately due to self-coordination of bacterial flagella. Finally, fluorescent microscopy is used to visualize induced *E.coli* cells (Figure 6c).

In summary, as shown in Figure 6, we are able to pattern two distinct monolayers of bacteria. One set of bacteria are responsible for actuation. The other set of bacteria can sense chemicals in the environment and fluorescent microscopy is used to estimate the chemical concentration in the environment. This immediately points to the feasibility of using estimates of GFP activity combined with electrokinetic actuation and ultraviolet radiation to steer MBRs toward biochemical sources.

VI. Discussion

Even though we demonstrated sensing for only TMG molecules, the experimental and modeling framework that we develop in this paper is meant as a model system for other biological systems with similar properties. Various different cell-based biosensors employing reporter genes have been developed to study a wide variety of analytes [19]. Provided that with a surface functionalization they can be immobilized on SU-8 microstructures, any such organism can be incorporated into this system. In addition to GFP, other reporter proteins such as bacterial luciferase or β-galactosidase can also be employed. As the cells are fixed on a planar geometry, we can use fluorescence imaging and bioluminescence.

The silanization process with a positively-charged APTES clearly enhances bacterial attachment however with this

method we could not form a high density bacterial carpet on our microstructures. Increasing the number of sensors is advantageous to obtain a more accurate read-out. To improve *E.coli* absorption, we are planning to extend out protocol by adding two more steps which includes biotinylation of *E.coli* cells and coating the surface of silanized microstructures with streptavidin molecules as suggested in [13].

The control capabilities of the MBRs can be extended by patterning cells on different parts of microstructures. Thanks to nonuniform distribution of charges, the angular velocity of the MBRs will become controllable using electric fields. It has been shown that a selective patterning of living bacteria can be generated by using microcontact printing process [30].

VII. Conclusion

In this paper, several important experimental techniques for building Micro Bio Robots (MBRs) are proposed and a theoretical framework for modeling and control of MBRs is presented. In particular, we proposed a method of controlling MBRs using self-actuation, DC electric fields and ultra-violet radiation, and developed experimentally validated mathematical model for MBRs. We also described the development of biosensors for the MBRs. The results presented in this paper have great potential. Our techniques can be used to fabricate, calibrate and transport MBRs with biosensing capabilities in microfluidic channels in a controllable fashion. Our future work will address the integration of bio-sensing and bio-actuation onboard the MBR.

VIII. Acknowledgment

References

[1] E. W. H. Jager, O. Inganas, and I. Lundstrom, "Microrobots for micrometer-size objects in aqueous media: potential tools for single-cell manipulation," *Science*, vol. 288, pp. 2335–2338, 2000.

[2] R. Dreyfus, M. L. Roper, H. A. Stone, and J. Bibette, "Microscopic artificial swimmers," *Nature*, vol. 437, pp. 862–865, 2005.

[3] M. Dauge, M. Gauthier, and E. Piat, "Modelling of a planar magnetic micropusher for biological cell manipulations," *Sens. Actuators A*, vol. 138, pp. 239–247, 2007.

[4] K. Vollmers, D. R. Frutiger, B. E. Kratochvil, and B. J. Nelson, "Wireless resonant magnetic microactuator for untethered mobile microrobots," *Appl. Phys. Lett.*, vol. 92, p. 144103, 2008.

[5] B. R. Donald, C. G. Levey, and I. Paprotny, "Planar microassembly by parallel actuation of mems microrobots," *J. Microelectromech. Syst.*, vol. 17, pp. 789–808, 2008.

[6] C. Pawashe, S. Floyd, and M. Sitti, "Multiple magnetic microrobot control using electrostatic anchoring," *Appl. Phys. Lett.*, vol. 94, p. 164108, 2009.

[7] L. Zhang, J. J. Abbott, L. Dong, B. E. Kratochvil, D. Bell, and B. J. Nelson, "Artificial bacterial flagella: Fabrication and magnetic control," *Appl. Phys. Lett.*, vol. 94, p. 064107, 2009.

[8] A. Ghosh and P. Fischer, "Controlled propulsion of artificial magnetic nanostructured propellers," *Nano Lett.*, vol. 9, pp. 2243–2245, 2009.

[9] T. G. Leong, C. L. Randall, B. R. Benson, N. Bassik, G. M. Stern, and D. H. Gracias, "Thetherless thermobiochemically actuated microgrippers," *Proc. Natl. Acad. Sci. USA*, vol. 106, pp. 703–708, 2009.

[10] M. S. Sakar, E. B. Steager, D. H. Kim, M. J. Kim, G. J. Pappas, and V. Kumar, "Single cell manipulation using ferromagnetic composite microtransporters," *Appl. Phys. Lett.*, vol. 96, p. 043705, 2010.

[11] N. Darnton, L. Turner, K. Breuer, and H. C. Berg, "Moving fluid with bacterial carpets," *Biophysical Journal*, vol. 86, pp. 1863–1870, March 2004.

[12] D. B. Weibel, P. Garstecki, D. Ryan, W. R. DiLuzio, M. Mayer, J. E. Seto, and G. M. Whitesides, "Microoxen: Microorganisms to move microscale loads," *Proc. Natl. Acad. Sci. U.S.A.*, vol. 102, no. 34, pp. 11 963–11 967, 2005.

[13] Y. Hiratsuka, M. Miyata, T.Tada, and T.Uyeda, "A microrotary motor powered by bacteria," *Proc. Natl. Acad. Sci. U.S.A.*, vol. 103, p. 13618, 2006.

[14] A. Sokolov, B. A. G. M. M. Apodaca, and I. S. Aranson, "Swimming bacteria power microscopic gears," *Proc. Natl. Acad. Sci. USA*, vol. 107, pp. 969–974, 2010.

[15] S. Martel, C. Tremblay, S. Ngakeng, and G. Langlois, "Controlled manipulation and actuation of micro-objects with magnetotactic bacteria," *Applied Physics Letters*, vol. 89, no. 23, p. 233904, December 2006.

[16] B. Behkam and M. Sitti, "Bacterial flagella-based propulsion and on/off motion control of microscale objects," *Applied Physics Letters*, vol. 90, no. 2, pp. 1–3, 2007.

[17] M. J. Kim and K. S. Breuer, "Use of bacterial carpets to enhance mixing in microfluidic systems," *Journal of Fluids Engineering*, vol. 129, pp. 319–324, 2007.

[18] E. Steager, C.-B. Kim, C. Naik, J. Patel, S. Bith, L. Reber, and M. J. Kim, "Control of microfabricated structures powered by flagellated bacteria using phototaxis," *Applied Physics Letters*, vol. 90, no. 26, p. 263901, 2007.

[19] S. Daunert, G. Barrett, J. S. Feliciano, R. S. Shetty, S. Shrestha, and W. Smith-Spencer, "Genetically engineered whole-cell sensing systems: Coupling biological recognition with reporter genes," *Chem. Rev.*, vol. 100, pp. 2705–2738, 2000.

[20] A. A. Julius, A. Halasz, M. S. Sakar, V. Kumar, H. Rubin, and G. J. Pappas, "Stochastic modeling and control of biological systems: the lactose regulation system of Escherichia coli," *IEEE Trans. Automatic Control*, vol. 53, no. 1, pp. 51–65, 2008, joint special issue with IEEE Trans. Circuits and Systems.

[21] A. A. Julius, M. S. Sakar, E. Steager, U. K. Cheang, M. J. Kim, V. Kumar, and G. J. Pappas, "Harnessing bacterial power in microscale actuation," in *Proceedings 41st IEEE Conf. Robotics and Automation*, Japan, May 2009.

[22] M. S. Sakar, E. B. Steager, D. H. Kim, A. A. Julius, M. J. Kim, V. Kumar, and G. J. Pappas, "Modeling, control and experimental characterization of microbiorobots," *International Journal of Robotics Research (in review)*, 2010.

[23] E. M. Ozbudak, M. Thattal, H. N. Lim, B. I. Shraiman, and A. van Oudenaarden, "Multistability in the lactose utilization network of *Escherichia coli*," *Nature*, vol. 427, pp. 737 – 740, February 2004.

[24] T. Miyashiro and M. Goulian, "Single cell analysis of gene expression by fluorescence microscopy," *Methods in Enzimology*, vol. 423, pp. 458–475, 2007.

[25] A. Cerf, J.-C. Cau, C. Vieu, and E. Dague, "Nanomechanical properties of dead and alive single-patterned bacteria," *Langmuir*, vol. 25, no. 10, pp. 5731–5736, 2009.

[26] D. C. Duffy, J. C. McDonald, O. J. A. Schueller, and G. M. Whitesides, "Rapid prototyping of microfluidic systems in poly(dimethlsiloxane)," *Anal. Chem.*, vol. 70, pp. 4974–4984, 1998.

[27] C. G. Cassandras and S. Lafortune, *Introduction to Discrete Event Systems*. Kluwer, 1999.

[28] A. Novick and M. Weiner, "Enzyme induction as an all-or-none phenomenon," *Proc. Natl. Acad. Sci. USA*, vol. 43, pp. 553–566, 1957.

[29] S. Takayama, J. C. McDonald, E. Ostuni, M. N. Liang, P. J. A. Kenis, R. F. Ismagilov, and G. M. Whitesides, "Patterning cells and their environments using multiple laminar fluid flows in capillary networks," *Proc. Natl. Acad. Sci.*, vol. 96, pp. 5545–5548, 1999.

[30] A. Cerf, J.-C. Cau, and C. Vieu, "Controlled assembly of bacteria on chemical patterns using soft lithography," *Colloids and Surfaces B: Biointerfaces*, vol. 65, pp. 285–291, 2008.